

Report No.
UCB/SEMM-2009/04

Structural Engineering
Mechanics and Materials

**Topology Optimization in
Microelectromechanical
Resonator Design**

By

Wei He, David Bindel and Sanjay Govindjee

December 2009

Department of Civil and Environmental Engineering
University of California, Berkeley

Topology optimization in microelectromechanical resonator design

Wei He · David Bindel · Sanjay Govindjee

Received: date / Accepted: date

Abstract A topology optimization problem in microelectromechanical resonator design is addressed in this paper. The design goal is to control the first several eigen-frequencies of a microelectromechanical resonator using topology optimization in order to improve the resonator's quality of resonance. The design variable is the distribution of mass in a constrained domain which we model via (1) the Simple Isotropic Material with Penalization Model and (2) the Peak Function Model. The overall optimization problem is solved using the Method of Moving Asymptotes and a Genetic Algorithm combined with a local gradient method. A numerical example is presented to highlight the features of the methods in more detail. The advantages and disadvantages of each method are discussed.

Keywords Topology optimization, Microelectromechanical resonator, Eigen-frequency, Moving asymptotes, Genetic algorithm

1 Introduction

Microelectromechanical (MEMS) resonators are important elements in the design of on chip signal processing systems for many next generation communication and sensing devices; see, for example, (Li et.al 2007). In the design of individual resonators, the so-called quality of resonance plays a major role. As

Wei He, Sanjay Govindjee
Department of Civil and Environmental Engineering
University of California, Berkeley, California, 94720
Tel.: +1-510-221-7940
Fax: +1-510-643-8928
E-mail: weihe@cal.berkeley.edu

David Bindel
Department of Computer Science
Cornell University, Ithaca, New York, 14853

pointed out in (Bindel and Govindjee 2005), it is desirable to control the location of resonant poles in such systems – with better resonance properties being obtained when the real parts of resonant frequencies are appropriately separated from each other. The control of this separation is essentially a topological optimization problem constrained by the equations of elastic wave propagation in a semi-infinite domain.

Topology optimization or generalized shape optimization of structures has been an active research area since at least the 1980s. One example that is frequently encountered in microelectromechanical system design is to find optimally compliant mechanisms (Saxena and Ananthasuresh 2000). The problem is usually to seek an optimal topology in a specified domain so that the structure can produce maximum displacements at some port. This is a typical optimization problem of specific entries of the global stiffness of a linearly elastic structure. A second important example occurs in car body design where optimal material layout is desired to reduce interior noise (Ma et al. 1993). This latter example is nearer to our area of interest as it involves the issue of dynamics.

The central task in topology optimization is to determine which geometric points in the design domain should be material points and which points should contain no material (i.e., are void). Based on a fine discretization of finite elements, one is faced with a large-scale “0/1” type integer optimization problem. By employing a material interpolation function, one can transform the discrete problem into a continuous problem which is relatively easier to solve. First we will review three common material distribution models and later we will focus on the use of two of them within our problem context.

An important but somewhat cumbersome material distribution model is the homogenization method (Bendsoe 1995; Bendsoe and Kikuchi 1988; Bendsoe 1989). In this method, each material point is looked on as a composite material consisting of an infinite number of infinitely small holes and material points which are periodically distributed. The effective material elasticity tensor at a point is given by

$$\mathbf{C}_{ijkl}(\mathbf{x}) = \frac{1}{|Y|} \int_Y \left[\mathbf{C}_{ijkl}(\mathbf{x}, \mathbf{y}) - \sum_{pq} \mathbf{C}_{ijpq}(\mathbf{x}, \mathbf{y}) \frac{\partial \chi_p^{kl}}{\partial y_q} \right] d\mathbf{y}. \quad (1)$$

Here, χ_p^{kl} is the microscopic displacement field solution to the (six) variational cell equilibrium equations:

$$\int_Y \sum_{pqij} \mathbf{C}_{ijpq}(\mathbf{x}, \mathbf{y}) \frac{\partial \chi_p^{kl}}{\partial y_q} \frac{\partial v_i}{\partial y_j} d\mathbf{y} = \int_Y \sum_{ij} \mathbf{C}_{ijkl}(\mathbf{x}, \mathbf{y}) \frac{\partial v_i}{\partial y_j} d\mathbf{y} \quad \forall \mathbf{v}, \quad (2)$$

where \mathbf{v} are Y -periodic displacement variations, $\mathbf{y} = \mathbf{x}/\epsilon$ represents fine scale positions and ϵ is a small parameter representing the ratio of fine scale to large

scale feature sizes. This theory, via the distribution of holes in the composite, gives a functional relationship between the density of material in the composite and the effective material properties. With this at hand, an optimal distribution of mass in the composite material in the design domain can be computed and the result can be interpreted as an optimal topology by thresholding.

Simple Isotropic Material with Penalization (SIMP) is a second common material interpolation model (Yin and Yang 2000). The elasticity tensor in this model is given by

$$\mathbf{C}_{ijkl}(\mathbf{x}) = [p(\mathbf{x})]^\eta \mathbf{C}_{ijkl}^0, \quad \eta > 1, \quad (3)$$

where $p(\mathbf{x})$, the design variable, is a density-like function and \mathbf{C}_{ijkl}^0 is the elasticity tensor of a given solid isotropic material. The parameter η can be used to penalize intermediate densities. The advantage of the SIMP model is that we can avoid the microstructure analysis of the homogenization model and the simplicity of the model can facilitate design. It also has been pointed out that when η is greater than or equal to three, the SIMP model obeys Hashin-Shtrikman bounds on the effective properties of composite materials (Yin and Yang 2000, Hashin and Shtrikman 1963).

The last model to be discussed here is the peak function model (Yin and Ananthasuresh 2001). In this model the elasticity interpolation is given as:

$$\mathbf{C}_{ijkl}(\mathbf{x}) = \sum_{m=1}^n \mathbf{C}_{ijkl}^m \exp \left[-\frac{[p(\mathbf{x}) - \mu_m]^2}{2\sigma_m^2} \right] + \mathbf{C}_{ijkl}^{void}, \quad (4)$$

where n is the number of material phases. With a small parameter σ_m , the exponential function in the expression is a continuous approximation to the δ -function. The advantage of this model is that the design variable, $p(\mathbf{x})$, can take any value between $-\infty$ and ∞ . Furthermore, this model can include multiple materials without increasing the number of design variables.

All these models have been successfully applied in the topology optimization of static problems, such as compliant mechanism design as mentioned above, tunnel support design, stiff structure design, etc. Further, the homogenization model has also been applied in the design of vibrating structures (Ma et al. 1995). In this paper, the SIMP model and the peak function model will be explored for use in dynamic problems of resonator optimization.

Choosing appropriate optimization algorithms is another important issue in topology optimization. Due to a very large number of design variables, conventional mathematical programming methods may result in a very poor efficiency in topology optimization. As a result, a kind of Optimality Criteria (OC) updating algorithm is often used instead (Bendsoe and Kikuchi 1988; Suzuki and Kikuchi 1991). It solves the necessary conditions for an optimal point iteratively. Even though it converges well in static problems, it

may not always work in dynamic problems. Thus some researchers have proposed a Modified Optimality Criteria (MOC) algorithm for frequency response optimization (Ma et al. 1993). This algorithm employs a shifted Lagrangian function to make a convex approximation and then solves the convex problem by using a dual method. In this paper, the Method of Moving Asymptotes (MMA) (Svanberg 1987) will be used as the main algorithm. MMA is based on a similar idea that deals with a non-convex problem by solving a sequence of convex approximations. It can be looked on as a further generalization of the widely used Convex Linearization method (CONLIN) (Fleury and Braibant 1986; Fleury 1989). In order to attempt to obtain a global optimum, Genetic Algorithms in conjunction with local refinement (Hybrid GA) will also be employed in this paper.

In summary, a simple but effective material distribution model and an efficient optimization algorithm along with a well-posed objective function form the key issues which must be addressed in topology optimization problems. In what follows we discuss our approach to each of these issues as they pertain to the problem of resonator quality optimization. This paper is focused on the control of the first several eigen-frequencies of a resonator and no energy dissipation is considered.

2 Material distribution models

The problem addressed here is to move the eigen-frequencies of a microelectromechanical resonator using topology optimization. Two material interpolation models are used in this paper: one is the SIMP model and the other is the peak function model. For the SIMP model the material interpolation function is repeated as follows:

$$\mathbf{C}(\mathbf{x}) = [p(\mathbf{x})]^{\eta_1} \mathbf{C}^0, \quad (5)$$

where p is the design variable at point \mathbf{x} and has a value between 0 and 1. To avoid singularities in finite element analysis, p should have a lower bound which is slightly greater than 0. The penalty factor η_1 is greater than 1. The above function has been used in static problems for a long time. For dynamics problems, a similar interpolation function is needed for the mass density:

$$\rho(\mathbf{x}) = [p(\mathbf{x})]^{\eta_2} \rho^0. \quad (6)$$

The only difference is that penalty factor η_2 has a different value than η_1 . The values of the two penalty factors need to be chosen so that the problem can be well approximated as the design variables approach their lower bound or upper bound.

For the peak function model, material interpolation functions for elastic moduli and mass density are defined as follows:

$$\mathbf{C}(\mathbf{x}) = \mathbf{C}^0 \exp \left[-\frac{[p(\mathbf{x})]^2}{\sigma_1} \right] + \mathbf{C}^{void} \quad (7)$$

$$\rho(\mathbf{x}) = \rho^0 \exp \left[-\frac{[p(\mathbf{x})]^2}{\sigma_2} \right] + \rho^{void}. \quad (8)$$

Similarly, \mathbf{C}^{void} and ρ^{void} are small positive numbers to avoid singularities. In this paper,

$$\mathbf{C}^{void} = \mathbf{C}^0 \times 10^{-15} \quad (9)$$

$$\rho^{void} = \rho^0 \times 10^{-16} \quad (10)$$

and σ_1 and σ_2 are small positive parameters so that the functions act as δ -functions. An advantage of the peak function model is that we do not need side constraints on the design variables.

3 Problem formulations

Based on a finite element discretization, where the ‘‘density’’-like design variables p_i are element-wise constant and the subscript i ranges from one to the number of elements in a specified design domain, $nelt$, the eigen-frequencies of the structure are then functions of p_i . In order to unify the two material distribution models, let us define another element-wise constant quantity:

$$\theta_i = p_i^{\eta_1}, \quad i = 1, nelt \quad (11)$$

for the SIMP model and

$$\theta_i = \exp \left[-\frac{p_i^2}{\sigma_1} \right], \quad i = 1, nelt \quad (12)$$

for the peak function model. Then the general problem can be formulated as:

$$\min_{p_i} \sum_{i=1, nelt}^n \left| \frac{\omega_k(p_i) - \bar{\omega}_k}{\bar{\omega}_k} \right| \quad (13)$$

subject to

$$g = \sum_{i=1}^{nelt} \theta_i (1 - \theta_i) = 0. \quad (14)$$

For the SIMP model, we further need to add bounds on the design variables:

$$0.05 \leq p_i \leq 1, \quad i = 1, nelt, \quad (15)$$

where 0.05 is used instead of 0 for lower bound to avoid singularities. In the objective function, the $\bar{\omega}_k$ are pre-specified target eigen-frequencies. By adjusting $\bar{\omega}_k$, we can cluster certain eigen-frequencies or make them well separated. The constraint implies that in each element the quantity θ_i must be either 0 or 1.

With this type of objective function, it is possible to obtain non-physically realizable checkerboard topologies. In order to avoid checkerboard patterns or one-node connected hinges in structures if four-node square finite elements are used, we need to add another constraint, as done in (Poulsen 2002):

$$H(\mathbf{p}) = 0, \quad (16)$$

where

$$H(\mathbf{p}) = \sum_{i,j} h(\theta_{i,j}, \theta_{i+1,j}, \theta_{i,j+1}, \theta_{i+1,j+1}) \quad (17)$$

is a descriptor function for one-node connected hinges. Here the sum effectively runs over all nodes and the double indexing of θ implies the four elements topologically connected to the node of concern. The local function

$$h(a, b, c, d) = m(a, b, d) \times m(a, c, d) \times m(b, a, c) \times m(b, d, c) \quad (18)$$

is defined at each node and

$$m(a, b, c) = |b - a| + |c - b| - |c - a|. \quad (19)$$

If we assume that θ_i has reached either 0 or 1 in each element, then each one-node connected hinge will make the local function $h = 16$. Note that local functions are non-negative and they can never be canceled out from node to node.

In summary, the problem formulation consists of Equations (13, 14, 16). If the SIMP model is used, the constraint shown in Equation (15) should be included as well.

4 Optimization algorithms

Two types of algorithms will be used to solve the optimization problems posed above. One is a Genetic Algorithm and the other is the Method of Moving Asymptotes (MMA) (Svanberg 1987; Svanberg 1995; Bruyneel et al. 2002). Due to the probable large size of the topology optimization problem, the conventional Genetic Algorithm must be combined with local refinement by gradient methods (Hybrid GA) to improve efficiency. In this paper, Hybrid GA is applied in conjunction with the peak function model. The constraint condition

is satisfied using a penalty method. The problem formulation is then slightly modified as:

$$\min_{\substack{p_i \\ i=1, nelt}} \sum_{k=1}^n \left| \frac{\omega_k(p_i) - \bar{\omega}_k}{\bar{\omega}_k} \right| + w_1 \times g + w_2 \times H. \quad (20)$$

The performance of the penalty method depends strongly on the choice of penalty factor and this actually constrains the wide application of the method. However, it is not a problem in our case because we clearly know how large each term on the right hand side of Equation (20) should be in a useful design. The first term is set based on the tolerance of the problem (about 0.05 in this paper). The second term g should be almost zero and the third term H must be zero. The penalty factors in this paper were chosen as:

$$w_1 = 10^5 \quad (21)$$

$$w_2 = 1. \quad (22)$$

The factors should be chosen such that the values of $w_1 \times g$ and $w_2 \times H$ are comparable. GA here is combined with the gradient method BFGS for local refinement. One or two iterations of BFGS were applied to each sampling point. This can greatly improve the performance of GA in the numerical experiments.

The second algorithm used here is MMA, which was particularly developed for structural optimization. It solves a sequence of convex approximating subproblems. Due to their convexity and separability, the subproblems can be efficiently solved by a dual method. This makes MMA a good choice for large scale problems in topology optimization. In our case, MMA is applied along with the SIMP model. The formulation was slightly modified as:

$$\min_{\substack{p_i \\ i=1, nelt}} \sum_{k=1}^n \left| \frac{\omega_k(p_i) - \bar{\omega}_k}{\bar{\omega}_k} \right| \quad (23)$$

subject to

$$g + H = 0 \quad (24)$$

$$0.05 \leq p_i \leq 1, \quad i = 1, nelt. \quad (25)$$

One difficulty in topology optimization is that the nearest local minima have to be avoided (Sigmund and Petersson 1998; Sigmund 1997). Local minima may make the MMA iteration stop very quickly and return an unacceptable result. Some techniques have been developed to deal with the problem (Sigmund and Petersson 1998; Sigmund 1997; Hilding 2000). The technique used here is a heuristic homotopy one. The constraint was relaxed first and then gradually made strict. As a result, many (non-feasible) intermediate ‘‘densities’’ would appear in the beginning of the optimization process, but this allowed the algorithm to avoid local minima and achieve better results to some extent. As the feasible domain becomes exact, all the intermediate ‘‘densities’’ go to their limiting values, either 0 or 1.

5 Sensitivity analysis

Both Hybrid GA and MMA require efficient gradient evaluations. Fortunately, for the problem which we address the gradient can be computed analytically. For the derivative of eigen-frequencies, consider the following standard eigen problem:

$$(\mathbf{K} - \lambda_n \mathbf{M})\phi_n = 0, \quad (26)$$

where $\lambda_n = \omega_n^2$ and \mathbf{K} and \mathbf{M} are global stiffness and mass matrices from a finite element discretization. The eigen-vectors will be assumed to be mass orthonormal. The sensitivity of λ_n to design variable p_i can be written as (Ma et al. 1995; Ma and Hagiwara 1991):

$$\begin{aligned} \frac{\partial \lambda_n}{\partial p_i} &= \phi_n^T \left(\frac{\partial \mathbf{K}}{\partial p_i} - \lambda_n \frac{\partial \mathbf{M}}{\partial p_i} \right) \phi_n \\ &= \phi_{n,i}^T \left(\frac{\partial \mathbf{k}_i}{\partial p_i} - \lambda_n \frac{\partial \mathbf{m}_i}{\partial p_i} \right) \phi_{n,i}, \end{aligned} \quad (27)$$

where $\phi_{n,i}$ stands for the component of the n th eigen-vector pertaining to the i th finite element and \mathbf{k}_i and \mathbf{m}_i denote the element stiffness and mass matrices, respectively. The sensitivity of the element stiffness and mass matrices can be calculated in a straight-forward manner:

$$\begin{aligned} \frac{\partial \mathbf{k}_i}{\partial p_i} &= \int_{\Omega_i} \mathbf{B}_i^T \frac{\partial \mathbf{D}_i}{\partial p_i} \mathbf{B}_i d\Omega \\ \frac{\partial \mathbf{m}_i}{\partial p_i} &= \int_{\Omega_i} \frac{\partial \rho_i}{\partial p_i} \mathbf{N}_i^T \mathbf{N}_i d\Omega. \end{aligned} \quad (28)$$

For plane stress problems, the material matrix in the i th element is given as:

$$\mathbf{D}_i = \begin{bmatrix} \frac{2\lambda_i\mu_i}{\lambda_i+2\mu_i} + 2\mu_i & \frac{2\lambda_i\mu_i}{\lambda_i+2\mu_i} & 0 \\ \frac{2\lambda_i\mu_i}{\lambda_i+2\mu_i} & \frac{2\lambda_i\mu_i}{\lambda_i+2\mu_i} + 2\mu_i & 0 \\ 0 & 0 & \mu_i \end{bmatrix}. \quad (29)$$

For the SIMP model

$$\lambda_i = \lambda^0 p_i^{\eta_1} \quad (30)$$

$$\mu_i = \mu^0 p_i^{\eta_1} \quad (31)$$

$$\rho_i = \rho^0 p_i^{\eta_2} \quad (32)$$

and

$$\frac{\partial \mathbf{D}_i}{\partial p_i} = \frac{\eta_1}{p_i} \mathbf{D}_i \quad (33)$$

$$\frac{\partial \rho_i}{\partial p_i} = \frac{\eta_2}{p_i} \rho_i. \quad (34)$$

For the peak function model

$$\lambda_i = \lambda^0 \exp \left[-\frac{p_i^2}{\sigma_1} \right] + \lambda^{void} \quad (35)$$

$$\mu_i = \mu^0 \exp \left[-\frac{p_i^2}{\sigma_1} \right] + \mu^{void} \quad (36)$$

$$\rho_i = \rho^0 \exp \left[-\frac{p_i^2}{\sigma_2} \right] + \rho^{void} \quad (37)$$

and

$$\frac{\partial \mathbf{D}_i}{\partial p_i} = -\frac{2p_i}{\sigma_1} \mathbf{D}_i \quad (38)$$

$$\frac{\partial \rho_i}{\partial p_i} = -\frac{2p_i}{\sigma_2} \rho_i, \quad (39)$$

where the terms with superscript “void” were ignored in the calculation of sensitivities.

It should be noted that the sensitivity calculation is different for repeated eigen-frequencies. In fact, the sensitivity analysis for repeated eigenvalues and the associated eigenmodes has been discussed frequently (Chen and Pan 1986; Dailey 1989; Juang et al. 1989; Mills-Curran 1988; Ma and Hagiwara 1994; Kenny and Hou 1994). Assume that ϕ_1 and ϕ_2 are a pair of eigenvectors associated with the (doubly) repeated eigenvalue λ . Then any linear combination of ϕ_1 and ϕ_2 , $y_1\phi_1 + y_2\phi_2$, is also the eigenvector associated with λ . The derivatives of a repeated eigenvalue λ can be obtained as the solution to the new (2 x 2) eigenvalue problem:

$$\left(\bar{\mathbf{K}} - \frac{\partial \lambda_j}{\partial p_i} \bar{\mathbf{M}} \right) \mathbf{y}_j = 0, \quad (40)$$

where

$$\begin{aligned} \bar{\mathbf{K}} &= [\phi_1, \phi_2]^T \left(\frac{\partial \mathbf{K}}{\partial p_i} - \lambda \frac{\partial \mathbf{M}}{\partial p_i} \right) [\phi_1, \phi_2] \\ \bar{\mathbf{M}} &= [\phi_1, \phi_2]^T \mathbf{M} [\phi_1, \phi_2] \end{aligned} \quad (41)$$

and $\mathbf{y}_j = [y_1, y_2]^T$ is a 2×1 vector.

We further need to calculate the sensitivities of the descriptor function which has been addressed in (Poulsen 2002). Consider the local function h defined in Equation (18), its derivative with respect to the 1st entry can be written as:

$$\begin{aligned} \frac{\partial h}{\partial a} &= \frac{\partial m(a, b, d)}{\partial a} \times m(a, c, d) \times m(b, a, c) \times m(b, d, c) + \\ &\quad \frac{\partial m(a, c, d)}{\partial a} \times m(a, b, d) \times m(b, a, c) \times m(b, d, c) + \\ &\quad \frac{\partial m(b, a, c)}{\partial a} \times m(a, b, d) \times m(a, c, d) \times m(b, d, c). \end{aligned} \quad (42)$$

Then the sensitivity of H to $\theta_{i,j}$ is:

$$\frac{\partial H}{\partial \theta_{i,j}} = \sum_{ii=\max(i-1,1)}^{\min(i,n_1-1)} \sum_{jj=\max(j-1,1)}^{\min(j,n_2-1)} h_{,k}(\theta_{ii,jj}, \theta_{ii+1,jj}, \theta_{ii,jj+1}, \theta_{ii+1,jj+1}), \quad (43)$$

where

$$k = i - ii + 2(j - jj) + 1 \quad (44)$$

and $h_{,k}$ stands for the derivative with respect to the k th argument. Here it is assumed that the design domain is discretized into $n_1 \times n_2$ square four-node finite elements. The sensitivity of H to design variable p_i can then be calculated by using the chain rule.

The sensitivity analysis of constraint (14) is trivial and omitted here.

6 Numerical examples

6.1 Description of problem

The example problem considered in this paper is the design of a square bounded microelectromechanical resonator. The goal is to adjust the first several eigenfrequencies using topology optimization. The white part in the center of Figure 1 is the design domain. The chocolate colored part represents existing material. The material of the resonator is poly-silicon, with the following properties:

$$E = 150 \text{ GPa} \quad (45)$$

$$\nu = 0.226 \quad (46)$$

$$\rho = 2330 \text{ kg/m}^3. \quad (47)$$

The structure has an in-plane vibration mode and a plane stress solid model is assumed in the whole structure. Four-node bi-linear elements were used to discretize the domain. The finite element analysis was performed using HiQLab (Bindel 2005). After discretizing the design domain into finite elements, one needs to determine the material density in each element. In other words, one needs to determine which elements are void and which are filled.

6.2 Validity of material distribution models

The validity of the material distribution models was examined first. For the models to be physically useful, the parameters η_1 , η_2 in the SIMP model or σ_1 , σ_2 in the peak function model must be chosen so that as θ goes to the

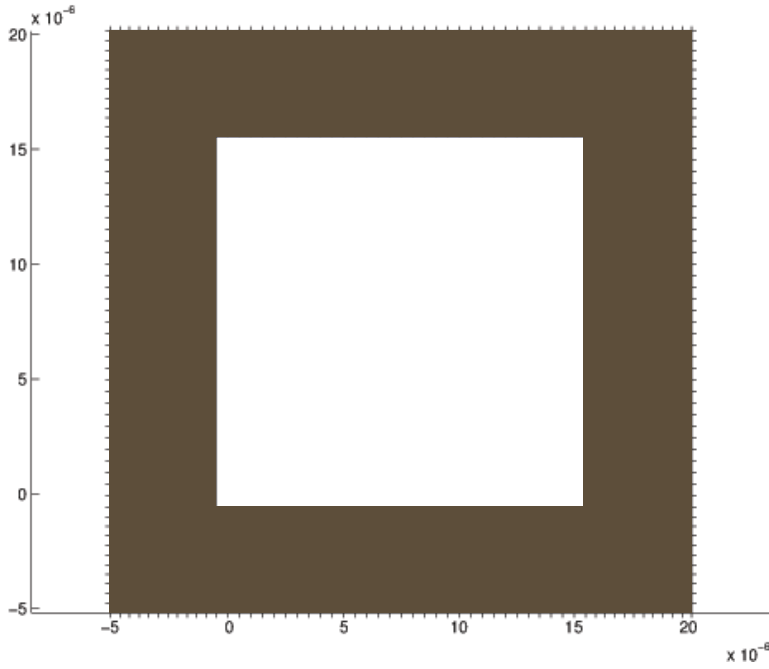


Fig. 1 Design domain of a microelectromechanical resonator (interior white part). Chocolate colored part represents existing material. Dimensions are in meters.

limiting values 0 or 1, the resulting eigen-frequencies approach those from a pure discrete problem. In this paper these parameters were set as:

$$\begin{aligned} \eta_1 &= 6 \quad , \quad \eta_2 = 11 \\ \sigma_1 &= 0.01 \quad , \quad \sigma_2 = 0.005. \end{aligned} \quad (48)$$

In Figure 2 and 3, the first several eigen-frequencies of the domain shown in Figure 1 were calculated from a pure discrete model for the cases of $\theta = 0$ (i.e., the interior part is void) and $\theta = 1$ (i.e., the interior part is completely filled), otherwise they were calculated from the continuous mass distribution models. Note that the case of $\theta = 0$ produces the eigenvalues solely associated with the boundary condition. We can see that the continuous mass distribution models converge well to the two limiting cases. This implies that each element can be simply interpreted as “on” or “off” as long as material density in it is close to 1 or 0.

6.3 Results by Hybrid GA

As the main advantage, Hybrid GA can find global optima, but it is still expensive as compared to MMA due to a very large number of objective evaluations.

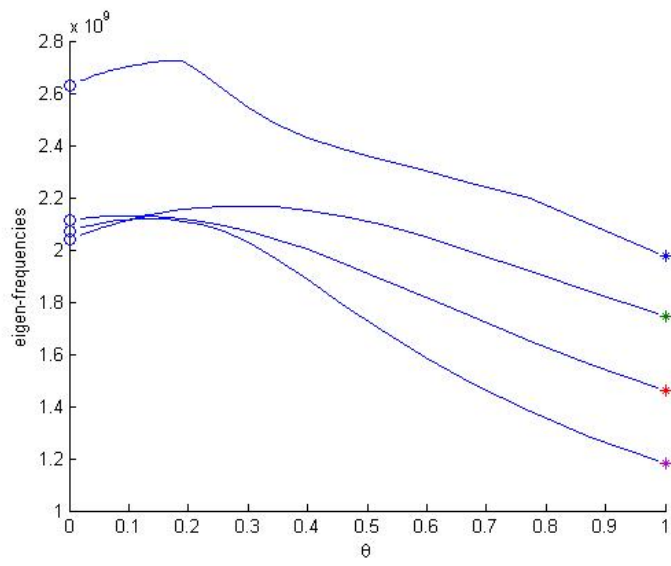


Fig. 2 Convergence of SIMP model λ_1 with pure discrete model used when $\theta = 0$ and $\theta = 1$.

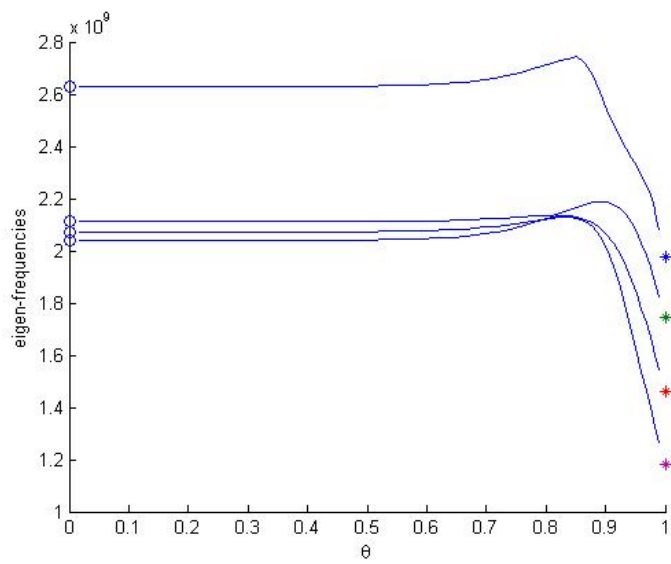


Fig. 3 Convergence of peak function model λ_1 with pure discrete model used when $\theta = 0$ and $\theta = 1$.

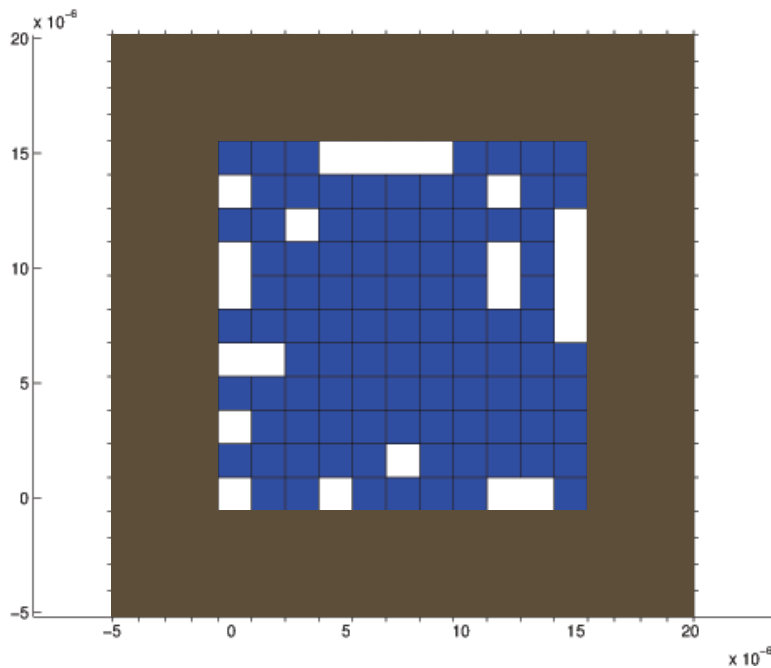


Fig. 4 Optimal topology by Hybrid GA (irregular but accurate in terms of objective function value). Dimensions are in meters.

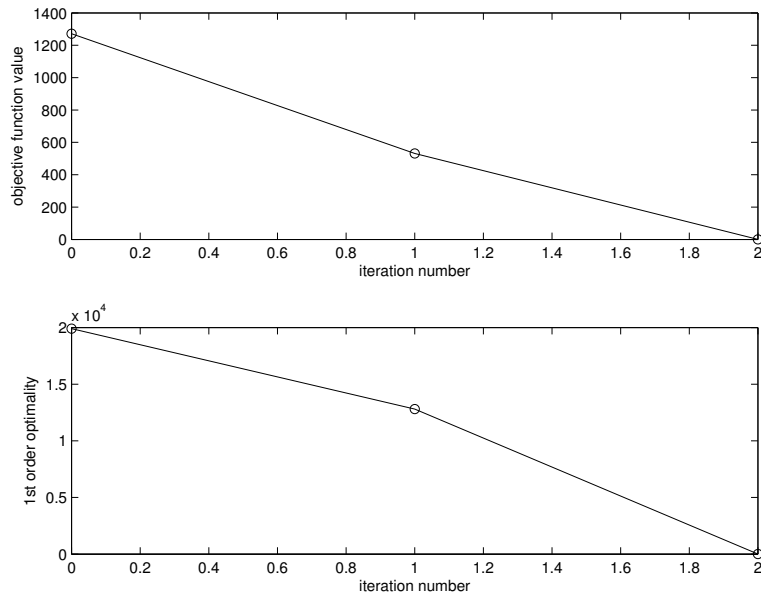
As mentioned before, in this paper Hybrid GA is applied in conjunction with the peak function material model. It can be applied on a coarse mesh resolution to get a preliminary result. Figure 4 shows an optimal topology obtained by Hybrid GA, where the goal was to cluster the first two eigen-frequencies around 1.04 GHz and the design domain was discretized into 121 finite elements. We obtained $\omega_1 = 1.0400$ GHz and $\omega_2 = 1.0434$ GHz. The result is ~~very~~ accurate in terms of frequencies, but it demonstrates an irregular topology and is certainly not good from the point of view of manufacturing.

6.4 Utility of local refinement in Hybrid GA

The efficiency of local refinement in Hybrid GA was examined as well. Starting from each sampling point in the previous example, one or two BFGS iterations were conducted. Figure 5 shows that local optimization highly improves the efficiency of GA. Both the objective function value and 1st order optimality decrease significantly in only five or six function evaluations, so it greatly saves overall computing time. Table 1 shows a comparison of the overall performance between conventional GA and Hybrid GA when the design domain

Table 1 Comparison between GA and Hybrid-GA.

	Conventional GA	Hybrid-GA
Function evaluations	11817	1060
Generations	500	10
Computing time	350 mins	115 mins
Objective function value attained	0.072	0.010

**Fig. 5** Efficiency of local refinement in Hybrid GA, with both objective function value (upper graph) and first order optimality (lower graph) going down significantly after two iterations of BFGS.

is discretized into 676 elements.

6.5 Results by MMA

As mentioned before, in this paper MMA is applied together with the SIMP material model. MMA is a local optimization algorithm, so it is prone to getting stuck in local minima. To avoid this, we have used a kind of continuation method mentioned above. By firstly applying a relaxed constraint and then making it stricter and stricter, instead of directly enforcing the exact constraint condition, one can achieve a satisfactory optimal design. In this case, the constraint function in (24) is rewritten as

$$g + H \leq \epsilon. \quad (49)$$

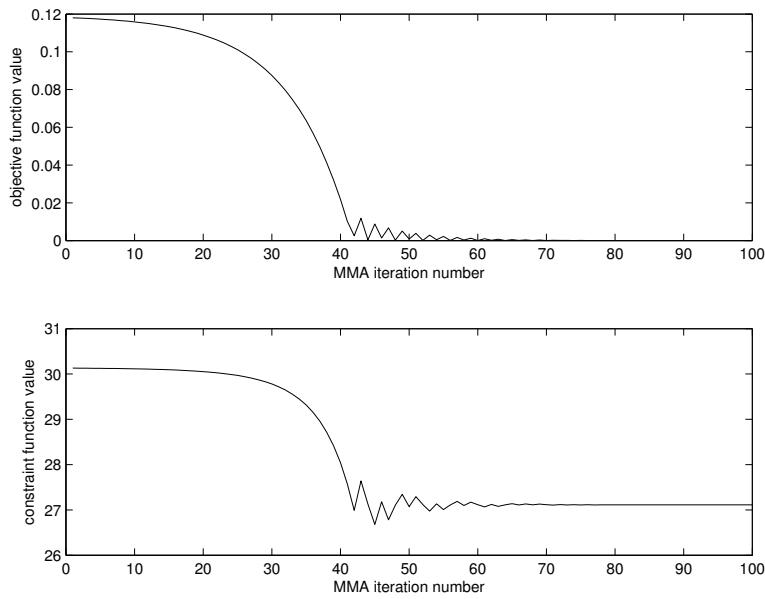


Fig. 6 First constrained problem solved by MMA, with small objective function value attained (upper graph) but large constraint function value (lower graph).

In the very beginning of the optimization process, ϵ is given a large positive value so that the constraint is essentially redundant. In the next step, the value of ϵ is lowered and a new sequence of MMA iterations is performed again to solve the new and stricter constrained problem. We repeat this procedure until the original constraint was satisfied, which means that all the intermediate variables reach their limiting values 0 or 1. Figure 6 shows how MMA works in the first step when the constraint condition is relatively weak; the upper curve plots the objective function values versus iteration number while the lower curve plots the constraint function values during the iterations. Figure 7 shows the case in the following step, where a smaller value of ϵ makes the optimal point in the first step infeasible. It will then converge to a new optimal point from outside the feasible space defined by the current ϵ . During this period, the objective function value has to go up but the constraint function value goes down. In Figure 7 it eventually stops at an interior point near the boundary. After solving a sequence of constrained optimization problems we can obtain a good optimal design. Figure 8 shows the terminal step where the objective function value can not go down inside the feasible domain, which implies that it converges to an optimal point that lies on the boundary. Both objective function value and constraint function value are reasonably small at the end of the process.

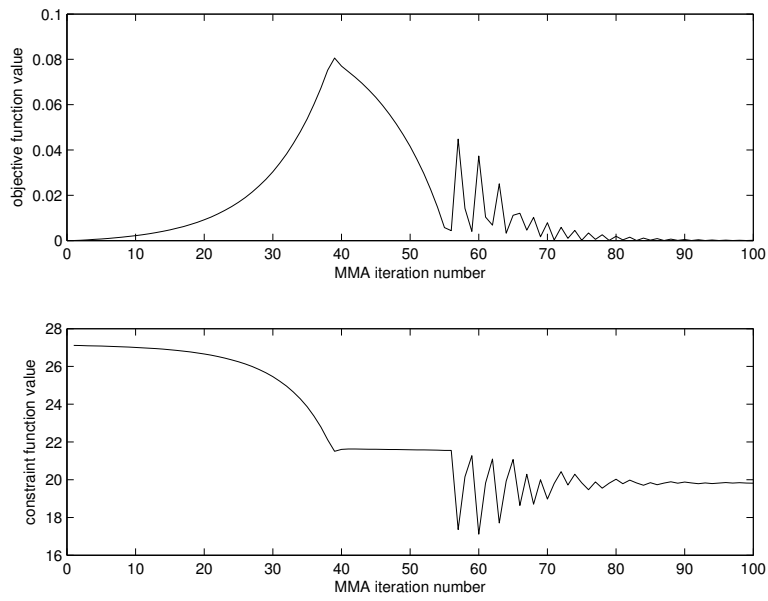


Fig. 7 Second constrained problem solved by MMA, with constraint function value going down (lower graph) but objective function value going up a little (upper graph).

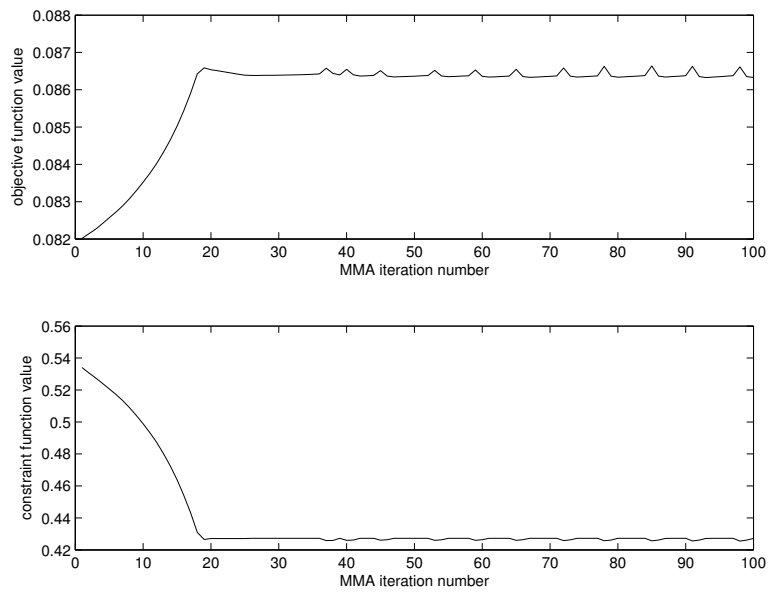


Fig. 8 Last constrained problem solved by MMA, with both objective function value (upper graph) and constraint function value being small (lower graph).

Some optimal topologies obtained using MMA are shown below. In these numerical examples there are 1024 elements in the design domain. The related parameters used in our MMA had the following value for each variable:

$$s_0 = 0.0001 \quad (50)$$

$$\bar{U}_i = 1.00 \quad (51)$$

$$\bar{L}_i = 0.05 \quad (52)$$

$$s_i = 0.8 \quad (53)$$

(refer to Svanberg 1987 for more detail of these parameters). These values were appropriate for our example problem as they made asymptotes close to iteration points and thus the program became more stable. This was necessary when the objective function value changed rapidly. For each value of ϵ , 100 iterations of MMA were executed to solve the corresponding constrained problem. In the next main iteration ϵ was decreased by a factor of 0.8 (i.e., $\epsilon_{i+1} = 0.8 \times \epsilon_i$ with i denoting main iteration number). The process was repeated until both the objective function value and the constraint function value became small enough. As the starting point of optimization, the material density was uniform over the whole domain and roughly equal to 0.5.

Figure 9 shows an optimal topology for setting the fundamental eigen-frequency. The target eigen-frequency is 1.5 GHz and the structure obtained has a fundamental eigen-frequency of 1.4 GHz. Figure 10 shows an optimal topology for clustering the first two eigen-frequencies around 1.04 GHz and we obtained $\omega_1 = \omega_2 = 1.03$ GHz. The corresponding eigen-modes are displayed in Figure 11 and Figure 12. Figure 13 shows the case where the first two eigen-frequencies are clustered around 1.04 GHz and well separated from the third one. The first five eigen-frequencies for this topology are

$$\begin{aligned} \omega_1 = \omega_2 &= 1.0230 \text{ GHz}, \\ \omega_3 &= 1.2390 \text{ GHz}, \quad \omega_4 = 1.6879 \text{ GHz}, \quad \omega_5 = 1.9348 \text{ GHz}. \end{aligned} \quad (54)$$

7 Summary and recommendations

We have presented a few options for topological optimization for eigen-frequencies of microelectromechanical resonators. As the first material distribution model, the peak function model was applied and the resulting optimization problem was solved using a Hybrid Genetic Algorithm. Local refinement was conducted using MATLAB's built-in function "fminunc" which implements the BFGS algorithm. The peak function model does not need side constraints for design variables, so we only need to solve an unconstrained optimization problem in local refinement and this improves efficiency. As the second material distribution model, the SIMP model was also applied and the resulting problem was solved using MMA. MMA can usually find an optimal structure with some

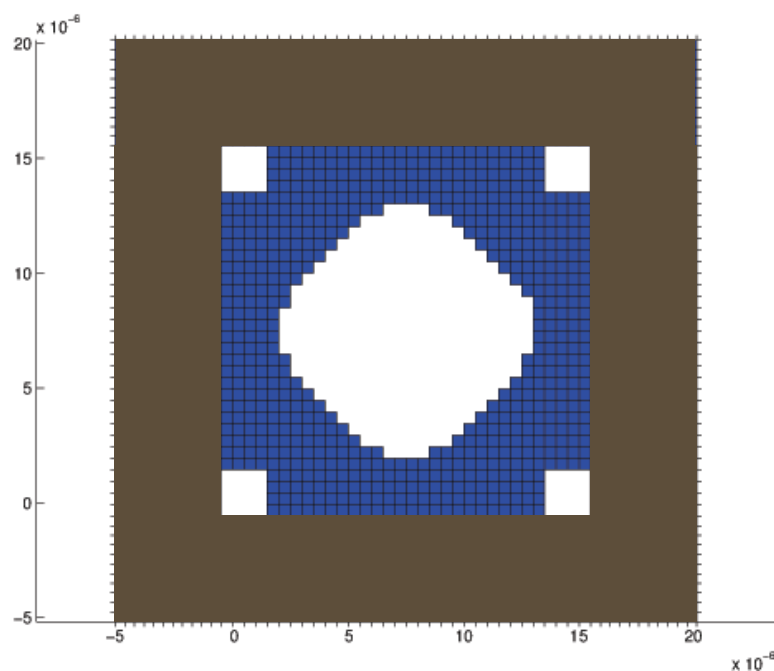


Fig. 9 Optimal topology for setting fundamental eigen-frequency to 1.4 GHz by MMA. Dimensions are in meters.

regularities, but it may stop at local minimum. Hybrid GA can lead to better result in terms of objective function values but the resulting structures are usually irregular due to its stochastic characteristic. Thus for our problem class, we find the MMA algorithm to be superior.

References

1. Beckers M (1999), Topology optimization using a dual method with discrete variables, *Structural Optimization*, 17:14-24
2. Bendsoe M (1989), Optimal shape design as a material distribution problem, *Struct. Optim.*, 1:193-202
3. Bendsoe M (1995), *Optimization of Structural Topology, Shape, and Material*, Springer, Germany
4. Bendsoe M, Kikuchi N (1988), Generating optimal topologies in structural design using a homogenization method, *Comp. Meth. Appl. Mech. Energ.*, 71:197-224
5. Bertsekas DP (1999), *Nonlinear programming*, Athena Scientific, Massachusetts, USA
6. Bindel D (2005), HiQLab: simulation of resonant MEMS, <http://www.cims.nyu.edu/dbindel/hiqlab/>
7. Bindel D, Govindjee S (2005), Elastic PMLs for resonator anchor loss simulation. *Int. J. Numer. Meth. Engrg.*, 64:789-818
8. Bruyneel M, Duysinx P, Fleury C (2002), A family of MMA approximations for structural optimization, *Struct. Multidisc. Optim.*, 24:263-276

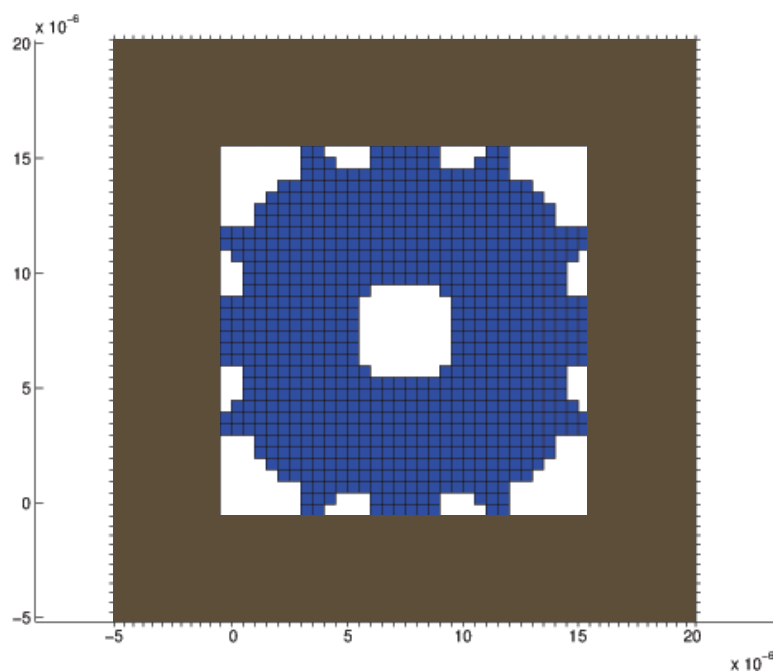


Fig. 10 Optimal topology for clustering the first 2 eigen-frequencies around 1.04 GHz by MMA. Dimensions are in meters.

9. Chen S, Pan H (1986), Design sensitivity analysis of vibration models by finite element perturbation, Proceedings of the 4th International Modal Analysis Conference, Los Angeles, California, USA, pp.38-43
10. Dailey R (1989), Eigenvector derivatives with repeated eigenvalues, AIAA Journal, 27:486-491
11. Duysinx P (1997), Layout optimization: A mathematical programming approach, DCAMM Report 540, Dept of Solid Mechanics, Technical of Denmark
12. Fleury C (1989), Efficient approximation concepts using 2nd order information, Int. J. Numer. Meth. Engrg, 28: 2041-2058
13. Fleury C, Braibant V (1986), Structural optimization - a new dual method using mixed variables, Int. J. Numer. Meth. Engrg, 23:409-428
14. Harber R, Jog C, Bendsoe M (1994), Variable-topology shape optimization with a control on perimeter, Advances in Design Automation, 69:261-272
15. Harber R, Jog C, Bendsoe M (1995), The perimeter method - a new approach to variable-topology shape optimization. In: N. Olhoff and G. Rozvany (ed) Proceeding of WCSMO-1, Structural and Multidisciplinary Optimization, Elsevier Science, Oxford, UK pp.153-160
16. Harber R, Jog C, Bendsoe M (1996), A new approach to variable-topology design using a constraint on the perimeter, Structural Optimization, 11:1-12
17. Hashin Z, Shtrikman S (1963), A variational approach to the theory of the elastic behaviour of multiphase materials, J. Mech. Phys. Solids, 11:127-140
18. Hilding D (2000), A heuristic smoothing procedure for avoiding local optima in optimization of structures subject to unilateral constraints, Struct. Multidisc. Optim., 20:29-36
19. Juang J, Ghaemmaghami P, Lim K (1989), Eigenvalue and eigenvector derivatives of a nondefective matrix, J. Guidance, 12:480-486
20. Kenny S, Hou G (1994), Approximate analysis for repeated eigenvalue problems with applications to controls-structures integrated design, NASA Technical Paper 3439

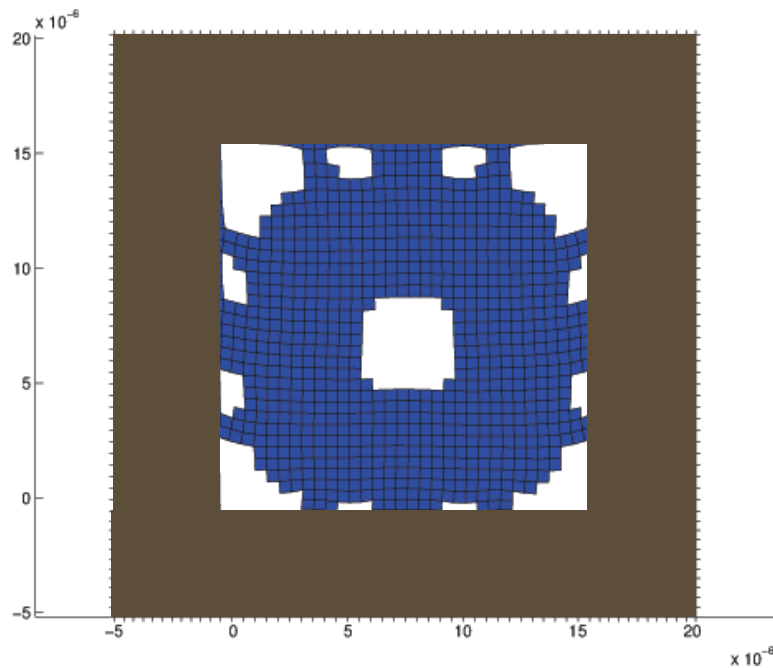


Fig. 11 First eigen-mode of structure in Fig. 10.

21. Li S, Lin Y, Ren Z, and Nguyen C (2007). An msi micromechanical differential disk-array filter. In Dig. of Tech. Papers, 14th Int. Conf. on Solid-State Sensors and Actuators (Transducers 07), pp.307-311
22. Ma Z, Hagiwara I (1991), Sensitivity analysis-methods for coupled acoustic-structural systems part I: modal sensitivities, AIAA Journal, 29:1787-1795
23. Ma Z, Hagiwara I (1994), Development of new mode-superposition technique for truncating lower and/or higher-frequency modes (application of eigenmode sensitivity analysis for systems with repeated eigenvalues), JSME Int. Journal, Series C, 37(1):7-13
24. Ma Z, Kikuchi N, Cheng H, Hagiwara I (1995), Topological optimization technique for free-vibration problems, J. appl. Mech. ASME, 62:200-207
25. Ma Z, Kikuchi N, Hagiwara I (1993), Structural topology and shape optimization for a frequency-response problem, Comp. Mech., 13:157-174
26. Mills-Curran W (1988), Calculation of eigenvector derivatives for structures with repeated eigenvalues, AIAA Journal, 26:867-871
27. Petersson J, Sigmund O (1998), Slope constrained topology optimization, International Journal for Numerical Methods in Engineering, 41:1417-1434
28. Poulsen T (2002), A simple scheme to prevent checkerboard patterns and one-node connected hinges in topology optimization, Struct. Multidisc. Optim., 24:396-399
29. Rozvany G, Bendsoe M, Kikuchi N (1995), Layout optimization of structures, Appl. Mech. Rev. ASME, 48:41-119
30. Saxena A, Ananthasuresh GK (2000), On an optimal property of compliant topologies, Struct. Multidisc. Optim., 19:36-49
31. Sigmund O (1997), On the design of compliant mechanisms using topology optimization, Mech. Struct. Mach., 25(4):493-524
32. Sigmund O, Petersson J (1998), Numerical instabilities in topology optimization: A survey on procedures dealing with checkerboards, mesh-dependencies and local minima, Struct. Optim., 16:68-75

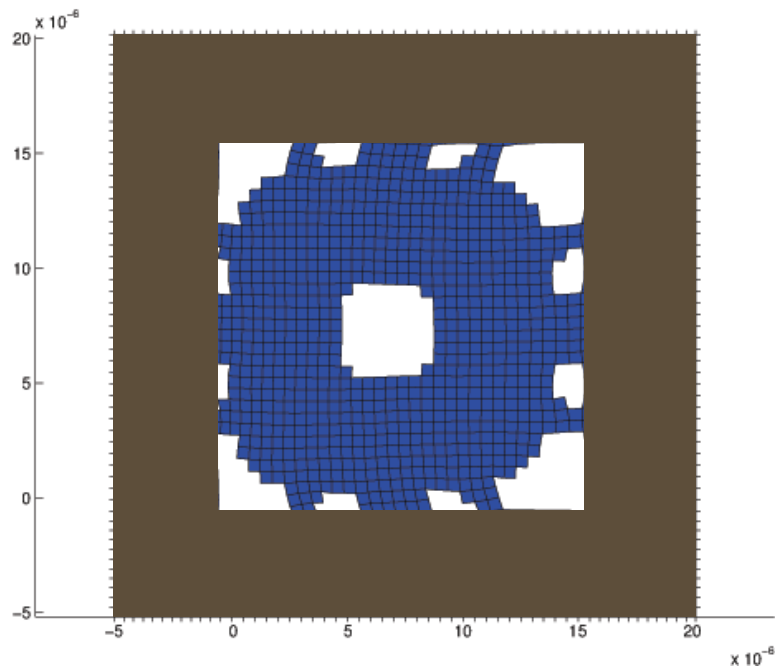


Fig. 12 Second eigen-mode of structure in Fig. 10.

33. Suzuki K, Kikuchi N (1991), A homogenization method for shape and topology optimization, *Comp. Meth. Appl. Mech. Engrg.*, 93:291-318
34. Svanberg K (1987), The method of moving asymptotes - a new method for structural optimization, *Int. J. Numer. Meth. Engrg.*, 24:359-373
35. Svanberg K (1995), A globally convergent version of MMA without linesearch. In: Rozvany, G.I.N.; Olhoff, N.(ed) *Proc. First World Congress of Structural and Multidisciplinary Optimization*, Oxford: Pergamon, pp. 9-16
36. Yin L, Ananthasuresh G (2001), Topology optimization of compliant mechanisms with multiple materials using a peak function material interpolation scheme, *Struct. Multidisc. Optim*, 23: 49-62
37. Yin L, Yang W (2000), Topology optimization for tunnel support in layered geological structures, *Int. J. Numer. Meth. Engrg.*, 47:1983-1996
38. Zhou M, Rozvany G (1991), The coc algorithm part II: topological, geometrical and generalized shape optimization, *Comp. Meth. Appl. Mech. Engrg.*, 89:309-336

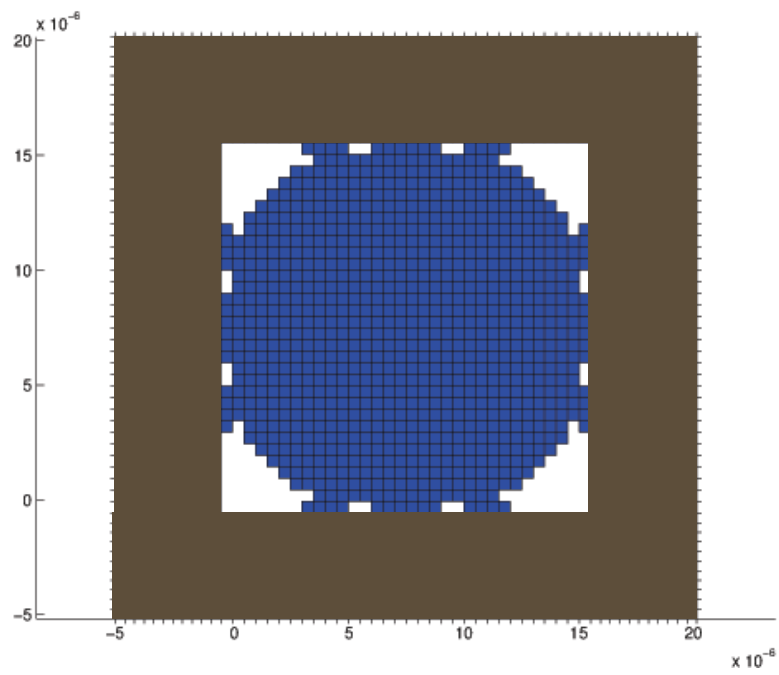


Fig. 13 Optimal topology for clustering the first 2 eigen-frequencies around 1.04 GHz and separating from others. Dimensions are in meters.